Voltammetry of Electroactive Oil Droplets: Electrochemically-Induced Ion Insertion, Expulsion and Reaction Processes at Microdroplets of *N,N,N′,N′*-Tetraalkyl-*para*-phenylenediamines (TRPD, R = *n*-Butyl, *n*-Hexyl, *n*-Heptyl and *n*-Nonyl)

Jay D. Wadhawan,[†] Russell G. Evans,[†] Craig E. Banks,[†] Shelley J. Wilkins,[†] Robert R. France,[‡] Neil J. Oldham,[‡] Antony J. Fairbanks,[‡] Bill Wood,[§] David J. Walton,[§] Uwe Schröder,[||] and Richard G. Compton*,[†]

Physical and Theoretical Chemistry Laboratory, Oxford University, South Parks Road, Oxford OX1 3QZ, United Kingdom, Dyson Perrins Laboratory, Oxford University, South Parks Road, Oxford OX1 3QY, United Kingdom, School of Science and the Environment, Coventry University, Priory Street, Coventry CV1 5FB, United Kingdom, and Institut für Chemie und Biochemie, Ernst-Moritz-Arndt Universität, Soldmanstrasse 16, 17489 Greifswald, Germany

Received: March 11, 2002; In Final Form: June 18, 2002

The electrochemistry of microdroplets, shown to be nearly monodisperse, of N,N,N′,N′-tetraalkyl-*para*-phenylenediamine oils (TRPD, R = *n*-butyl, *n*-hexyl, *n*-heptyl, and *n*-nonyl) immobilized on a basal plane pyrolytic graphite electrode and immersed into aqueous electrolyte solution is studied using cyclic voltammetry. Upon oxidation of the TRPD droplet to the cation radical $TRPD^{+\bullet}$, anion uptake from, or cation loss into the aqueous solution takes place, so as to maintain electroneutrality within the oily deposit. The former process is shown to produce an ionic liquid, with the anion insertion taking place at the triple phase boundary of electrode |TRPD oil| aqueous electrolyte; the latter process, in contrast, takes place at the interface between the two immiscible liquids, and with two-thirds-order kinetics. The possibility of a chemical reaction taking place between the electrogenerated and inserted ions at the three-phase junction, viz. redox-catalysis or otherwise, is illustrated via reference to two systems (azide and iodide).

1. Introduction

Over the past decade, there has been a considerable increase in the use of room-temperature ionic liquid materials as solvents for organic syntheses.[1,2] The primary reasons for this has been that their use may incur a selectivity in chemical reaction, while providing a significant "greening" of the synthetic procedure when compared with conventional solvents.[1,2] Ionic liquids are well suited for electrochemical processes under a plethora of reaction conditions, since they are ion conductors[3] and have zero volatility.[1] Recent technological applications include their use as dielectric materials in capacitors[4] and field-effect transistors,[5] as energy-storage media in batteries,[6] and in solar cell applications.[7]

Over the last five years, our group has pioneered the electrochemical generation of ionic liquids formed via electrochemically induced ion insertion into an oily material immobilized on an electrode surface.[8−17] Electroinsertion processes in solid materials, especially for the case of ion insertion into microcrystalline materials attached to electrode surfaces are technologically attractive; examples include the use of these processes as functional materials in rechargeable batteries, in electrochromic systems, in electrocatalysis and in the development of new types of sensor technology.[18,19] Furthermore, Abbott and Rosslee have reported a method for electrochemical control of the self-assembly of a redox surfactant on an electrode, and have used this to illustrate microscale separations.[20] In other work, Kontturi *et al.*[21] have studied the electrochemistry of lipid monolayer liquid|liquid interfaces as a model for the uptake of drugs into target cells. The method of depositing microdroplets of a molecular liquid onto a graphitic electrode and then investigating the voltammetric responses when the electrode is placed in aqueous electrolyte media, has been shown to broaden the range of methods for the study of redox chemistry at liquid|liquid interfaces[8−17] because, in contrast to the case of adsorbed monolayers being reduced or oxidized, the redox conversion of bulk oils requires the uptake or expulsion of ions dictated by the requirement of electroneutrality. This means that the redox process is very sensitive to the nature and the concentration of ions in the surrounding aqueous environment.[8,9,11,16] Furthermore, we have shown that the careful design of the neutral oily precursor can control the ion insertion,[10] encouraging the development of novel solution-based electroanalytical techniques.[22−27]

The large majority of our work has focused upon the oxidation of microdroplets of N,N,N′,N′-tetrahexyl-*para*-phenylenediamine (THPD). This material is a water-insoluble yellow-brown liquid, whereas the lower molecular weight derivative N,N,N′,N′-tetramethyl-*para*-phenylenediamine (TMPD) is a solid with a greater solubility in water. The hexyl chains confer the material with a hydrophobic character, rendering it immiscible with water. This material, when deposited in the form of microdroplets on an electrode surface, can undergo two one-electron oxidative processes, each accompanied by anion, X^-, uptake

* To whom all correspondence should be addressed. E.mail: compton@ermine.ox.ac.uk. Tel: +44 (0) 1865 275 413, Fax: +44 (0) 1865 275 410.
[†] Physical and Theoretical Chemistry Laboratory, Oxford University.
[‡] Dyson Perrins Laboratory, Oxford University.
[§] School of Science and the Environment, Coventry University.
[||] Institut für Chemie und Biochemie, Ernst-Moritz-Arndt Universität.

10.1021/jp020679o CCC: $22.00
Published on Web 08/24/2002

$$\mathrm{THPD(oil)} + \mathrm{X^-(aq)} - \mathrm{e^-} \rightleftarrows [\mathrm{THPD^{+\bullet}X^-}](\mathrm{oil}) \quad \text{(A)}$$

$$[\mathrm{THPD^{+\bullet}X^-}](\mathrm{oil}) + \mathrm{X^-(aq)} - \mathrm{e^-} \rightleftarrows [\mathrm{THPD^{2+}X_2^-}](\mathrm{oil}) \quad \text{(B)}$$

The first process is chemically reversible for anions such as hexafluorophosphate, perchlorate, thiocyanate, and nitrate,[8,9] and has also been shown to yield fully reversible voltammetric responses for chloride and bromide at slightly elevated temperatures.[11] Schröder and co-workers[17] have shown that the potential of insertion of these ions is governed by the Gibbs energy of transfer of the electrolyte anions: if the free energy for the anion transfer is low (typically < ca. 40 kJ mol^{-1}), the transfer of anions across the liquid|liquid interface takes place upon electrooxidation of THPD, with the more hydrophobic anion inserting more easily (i.e., at more negative potentials); anions with high transfer energies (such as fluoride and sulfate) do not enter the organic phase. Instead, upon electrooxidation, the $THPD^{+\bullet}$ radical cation is transferred from the oil phase to the aqueous solution, leading to a diminution of the current|voltage behavior, due to loss of material from the electrode. On the other hand, many anions such as acetate do not undergo reversible electroinsertion under the same conditions.[8,9,11] In this paper, we shall only consider the first oxidation of the TRPD oil because, in the presence of water, the $TRPD^{2+}$ dication may undergo hydrolysis.[28]

In earlier papers we have aimed to discover the mechanism for the insertion process. We have proposed three models in which the electrochemical reactions could take place.[12a] These are summarized in Figure 1. In model a, the electrochemical process is assumed to commence from the electrode|oil droplet interface. This model requires the prior partitioning of electrolyte into the deposit, and it is assumed that little or no polarization across the droplet, or across the droplet|aqueous electrolyte interface occurs. In model b, the droplet deposit is assumed to act as an insulator except for the oil|aqueous electrolyte interface, which is assumed to rapidly conduct electrons. The electrochemical conversion of the deposit in this case commences from the oil|aqueous electrolyte interface, and the diffusion of ion pairs is the dominant transport mechanism. In the third scheme, model c, electron conduction across the oil|aqueous electrolyte interface is slow. In this case, anion insertion only occurs in the region of the three-phase junction of electrode|oil|electrolyte. Numerical modeling using a finite element technique[12a,29] was used to characterize mechanistically the three models. Subsequently,[12b] we examined the experimental results in the light of the numerical simulation, and observed that the overall mechanism for insertion, especially at higher scan rates, is consistent with model c (electrochemical insertion process taking place at the three-phase boundary). Additionally, we observed that the insertion process was in absolute value too fast for it to be controlled by diffusion alone, suggesting that a Marangoni-type convective effect[30] is possibly additionally operative.[11,12b] A recent paper[31] has illustrated that for the case of microparticles of a redox-active solid immobilized at an electrode surface, ion insertion takes place directly at the triple phase boundary.

The aim of this paper is to examine three types of electrochemically induced processes at electrodes modified with microdroplets and thin films of N,N,N′,N′-tetraalkyl-*para*-phenylenediamines (TRPD, R = *n*-butyl, *n*-hexyl, *n*-heptyl, and *n*-nonyl). All four of these compounds are room-temperature liquids.[17] We first look at the electrochemically induced insertion of ions into these compounds and confirm this takes place at the triple phase boundary (model c). Second, we investigate the electrochemically induced ion dissolution process, whereby the $TRPD^{+\bullet}$ radical cation is expelled from the oil phase. We show that for this to take place, there must be rapid charge transport over the oil|aqueous electrolyte interface (model b type behavior). Third, we consider electrolytes that give essentially irreversible current|potential behavior. We suggest that this results from a nucleophilic reaction process occurring at or near the triple phase junction.

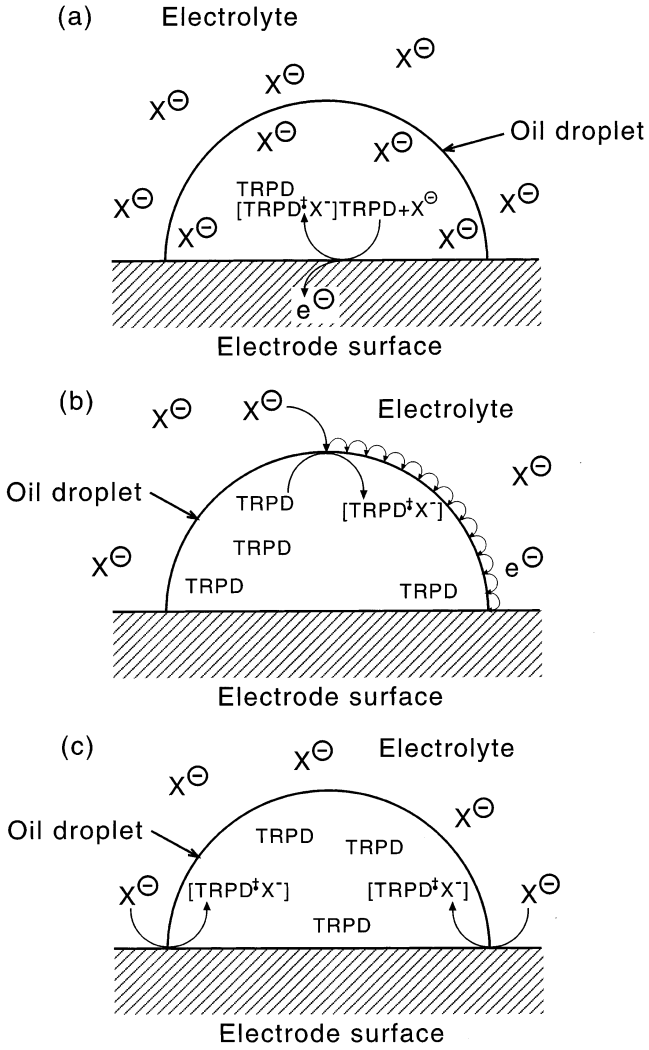

Figure 1. Schematic illustrations of the three possible methods for anion insertion upon oxidation of the TRPD deposit.

2. Experimental Section

2.1 Chemical Reagents. The N,N,N′,N′-tetraalkyl-*para*-phenylenediamines (TRPD, R = *n*-butyl, *n*-hexyl, *n*-heptyl, and *n*-nonyl) were synthesized following a literature procedure; their characteristics have been reported in earlier work.[8,17] For the deposition procedure, acetonitrile (Fisons, dried and distilled) was used without further purification. Electrolyte reagents, KSCN (Fisons), $NaClO_4$, KPF_6, KOCN, NaOAc, disodium tartrate, and $KAsF_6$ (all Aldrich), $AgClO_4$, KNO_3, $MgSO_4$, NaN_3, KF, KCl, KBr, KI, KIO_3, and $Na_2C_2O_4$ (all BDH) were of the purest commercially available grade. Water, with a resistivity of not less than 18 MΩ cm, used to make the electrolyte solutions was taken from an Elgastat system (USF, Bucks., UK). All solutions were degassed with argon or nitrogen (BOC Gases, Guildford, Surrey, UK) for at least 10 min prior

to experimentation. Unless otherwise stated, experiments were conducted at 20 ± 2 °C.

2.2 Instrumentation. Electrochemical experiments were conducted in a conventional three-electrode cell, using a 4.9 mm diameter basal plane pyrolytic graphite (bppg, Le Carbone Ltd., Sussex, UK) working electrode, a platinum or nickel wire counter electrode and a saturated calomel reference electrode (SCE, Radiometer, Copenhagen, Denmark). Although this reference electrode can be sensitive to high concentrations of perchlorate anions (due to the precipitation of $KClO_4$ at the calomel frit), the resulting potential drift was minimized by employing short exposure time in perchlorate solutions. Gold ring electrodes were constructed by encasing both external and internal walls of a gold tube (2 mm o.d., 1.8 mm i.d., Goodfellow Cambridge Ltd., UK) in PTFE. Electrochemical data were recorded using either an Oxford Electrodes analogue potentiostat (Oxford, England) connected to a Lloyd PL3 chart recorder (JJ Instruments, Southampton, UK), or a commercially available computer-controlled potentiostat (Autolab PGSTAT30 or PGSTAT20, Eco Chemie, Utrecht, Netherlands), utilizing a small potential step size.[15] The bppg working electrode was modified with TRPD microdroplets by solvent evaporation of an aliquot of 1 mM TRPD/MeCN stock solution. The electrode was cleaned by rinsing with acetonitrile, and occasionally renewed by polishing on carborundum paper (P1000 grade) immediately prior to experimentation.

For sono-emulsion experiments, a small volume cell was used as described previously.[32] The ultrasound generator employed was a VCX400 model sonic horn (Sonics and Materials, USA) equipped with a 3 mm diameter stepped titanium alloy probe emitting at 20 kHz. Electrochemical experiments were conducted using a 1 mm disk shaped Pt electrode in a conventional sonoelectrochemical cell,[32] employing a Pt counter electrode and a silver wire quasi-reference electrode.

Analysis of the TRPD droplets by SEM (scanning electron microscopy) was carried out using a Cambridge Stereoscan scanning electron microscope. The samples were gold sputter coated prior to analysis. Analysis of the TRPD deposits using Maldi TOF mass spectrometry was undertaken as used previously; samples were collected by dissolving the TRPD electrode deposit in 1 mL of cry ether.[11] Further analysis using positive ion electrospray (ESI+) was undertaken, using a VG BioQ quadrupole mass spectrometer equipped with a "Z-Spray" electrospray source. The samples were injected in methanol at a flow rate of 30 μL min^{-1}. The capilliary and cone voltages were 3.1 kV and 31 V, respectively. Spectra were acquired in the continuum mode over a scan range of *m*/*z* 200 to *m*/*z* 800 at a rate of 0.3 scans s^{-1}.

3. Results and Discussion

We begin by characterizing the bppg electrode surface modified (as described in the Experimental section) with microdroplets of TRPD oils.

3.1 Immobilization of TRPD Microdroplets: Size Distribution and Voltammetric Characteristics on Immersion in Aqueous Electrolyte. The hydrophobic nature of the TRPD liquids permits the interrogation of their redox chemistry via immobilization of microdroplets of the oily depolarizer onto the electrode surface, as undertaken in previous work.[8−17] Work of a similar nature undertaken primarily by Scholz and coworkers, involves the deposition of a liquid droplet (containing a dissolved redox-active solid) of known volume (but not geometry) on the electrode surface (usually paraffin-impregnated graphite).[33−37] Figure 2 shows a schematic representation of the modified electrode surface. In previous work, we have assumed that the microdroplets, formed via evaporation of a volatile solvent, nucleate in troughs present on the rough basal plane pyrolytic graphite electrode surface.[12b] This view is indirectly supported by the formation of a single large droplet, when the deposition procedure takes place on a smooth, polished electrode surface, such as polished glassy carbon or platinum. It is likely that the formation of microdroplets in this manner occurs via an "Ostwald Ripening" process: the greater the quantity of material deposited, the larger the final droplet size. In our previous work,[11,12] we have based our estimations of the most likely droplet diameter (ca. 1 μm for ca. 10 nmol THPD deposited) on the size of the striations in the basal plane pyrolytic graphite electrode surface. In other work, we have shown that because the ionic liquid generated by the electroinsertion process absorbs electron beams very efficently,[9] the easiest way to image the droplet deposit is via optical microscopy[8] (the radical cations are strongly colored blue, with absorption maxima < 400 nm, and at 550−660 nm[13,15]). We now report an alternative method for the determination of the droplet size distribution, based on the well-known use of *para*-phenylenediamine as a photographic developer. Experiments were conducted where the TRPD modified electrode was dipped for a few seconds into a 0.1 M aqueous solution of silver perchlorate. This allows a chemical reaction to take place in which the silver ions oxidize the TRPD species

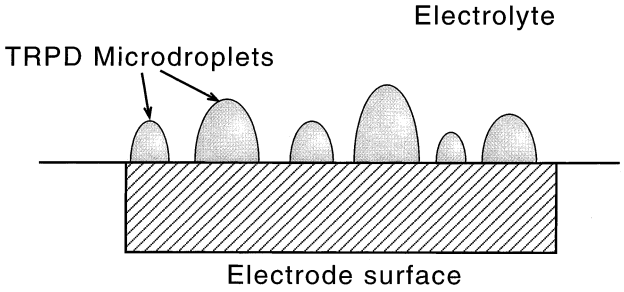

Figure 2. Schematic illustration of the electrode surface modified with a random array of microdroplets of TRPD.

$$\mathrm{TRPD(oil)} + \mathrm{Ag^+(aq)} + \mathrm{ClO_4^-(aq)} \rightarrow [\mathrm{TRPD^{+\bullet}ClO_4^-}](\mathrm{oil}) + \mathrm{Ag(s)} \quad \text{(C)}$$

The chemical reaction takes place at the oil/aqueous electrolyte interface, consequently forming metallic silver at the TRPD droplets. Figure 3a illustrates typical SEM images of these surfaces, and Figure 3b shows the measured size distributions for two amounts of THPD immobilized upon the bppg electrode surface. (The distributions have been obtained from undertaking a statistical analysis of four SEM photographs for both quantities of THPD.) We see that in both cases, the microdroplets are almost monodispersed, with average size distributions of 4.2 μm (for 4 nmol THPD deposited, standard deviation 1.1 μm), and 20.6 μm (for 40 nmol THPD deposited, standard deviation 6.5 μm). Furthermore, as anticipated in earlier work,[12b] it can be seen that the droplets are mainly formed within the troughs of the bppg electrode, i.e. "nucleation" of the TRPD oils takes place where the electrode surface energy is locally high. This may explain the formation of ensembles of microdroplets observed over the bppg surface.

As an aside we note that process C produces the radical cation of the TRPD oil immobilized upon the electrode surface. It follows that the potentiostating of the electrode at 0 V vs SCE (a potential known to reduce the $TRPD^{+\bullet}$ cation radical, but

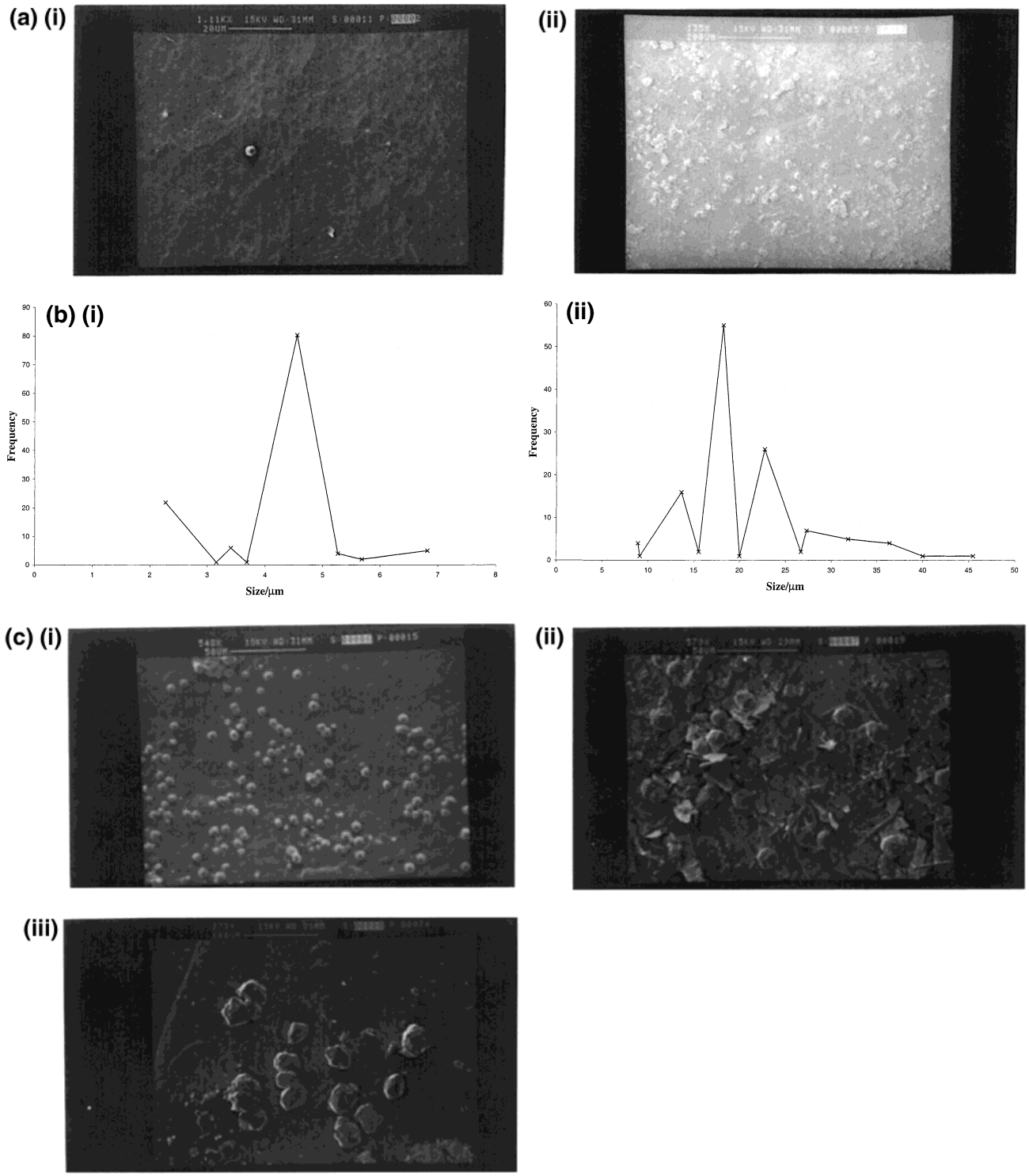

Figure 3. (a) SEM image of (i) 4 nmol, and (ii) 40 nmol of THPD deposited on a bppg electrode and immersed in $AgClO_4$ for 10 s (at open circuit potential). (b) Measured droplet distributions for the two coverages indicated in (a). (c) Evidence for reaction at the triple phase boundary: SEM images of 4 nmol THPD deposits on bppg electrodes and electrolytsed at 0 V vs SCE for (i) 10 s, (ii) 60 s, and (iii) 5 min.

not Ag^+) permits the electrocatalytic reduction of silver. Figure 3c illustrates SEM images of the surface after the applied voltage has been stepped from 0.4 V vs SCE to 0 V vs SCE for variable times ((i) 10 s, (ii) 60 s, (iii) 5 min). Comparison of Figure 3c(i) with the images in Figure 3a shows that the electrocatalytic silver deposition takes place rather at the three-phase boundary of electrode|oil|electrolyte, (as observed by the formation of silver microrings, with average i.d. of 2.8 μm and average o.d. of 5.7 μm) providing direct and unambiguous evidence that this is where the electrochemical reduction of $TRPD^{+\bullet}$ to TRPD initially takes place. This prima facia evidence for electrochemical reaction at the triple phase junction compares well with the optical images of THPD oxidation at a siliconised ITO electrode reported by Marken (Figure 6, reference 8). The potentiostatic electrocatalytic depostion of silver at longer times (Figure 3c, parts (ii) and (iii), shows that silver nucelation then takes place over the oil droplet (as the presence of a conductive silver layer increases the size of the three-phase junction), causing the

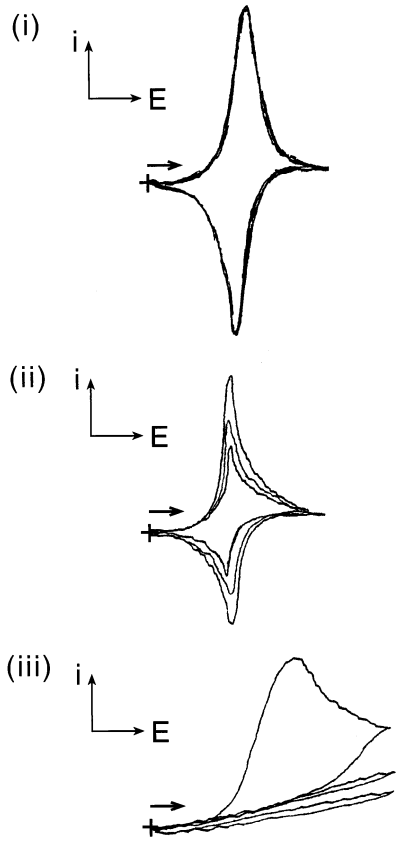

Figure 4. Schematic illustration of the three types of voltammogram observed. (i) Anion insertion, case (i) behavior; (ii) cation expulsion, case (ii) behavior; (iii) ionic reaction at the triple phase boundary, case (iii) behavior.

formation of larger silver microparticles (with average size of 32.1 μm, and s.d. of 9.9 μm), and, in some cases, clusters, Figure 3c(iii).

We next turn to the current|voltage behavior of TRPD microdroplets in various aqueous electrolyte solutions. Several characteristic voltammetric profiles have been reported for the case of microdroplets of a redox-active liquid deposited upon an electrode surface, and immersed into aqueous electrolyte.[8−11,15,35] Figure 4 illustrates schematic voltammograms, corresponding to a single oxidation of the liquid for the case of N,N,N′,N′-tetraalkyl-*para*-phenylenediamines immobilized upon basal plane pyrolytic graphite electrodes. It is clear that three distinct types of *i*|*E* behavior exist: (i) the voltammetry is reproducible over many cycles, with narrow peak shapes and with a small separation between the oxidation and reduction peaks, implying both chemical and electrochemical reversibility; (ii) the voltammetry is as in (i), except the signals are not stable over consecutive scans, the signal constantly diminishes over several cycles; (iii) the voltammetry is apparently chemically irreversible, there is a peak in the current in the initial voltage sweep direction, but this is lost when scanning in the reverse direction and no peaks appear in any subsequent scans. In Table 1, we have categorized the voltammetry of the four TRPD liquids in the presence of various anions into one of the three general cases (i), (ii), or (iii) indicated above.

In the following, we show that these three distinct voltammetric behavior correspond to three different types of electrochemical process: (i) anion insertion at the triple phase junction, (ii) cation expulsion, i.e., dissolution, at the liquid/liquid interface, and (iii) chemical reaction of ions (inserted and electrogenerated) at or near the three phase boundary for the three respective general cases outlined above. We will see how different anions can be categorized as "inserters", "expellers", or "reactors". Within each general case, we show that there are subtle differences between each ion, depending upon the ion hydrophobicity (q.v., ref 17 for thermodynamic arguments). We further consider the mechanism of the electrochemical process, and establish that this takes place at the triple phase boundary (for the case of insertion, and reaction), *or* at the oil|electrolyte interface (for the case of dissolution).

3.2 Case (i): Electrochemically-Induced Ion Insertion Processes. This case is the "model" case that has been considered in previous papers.[8−17] The voltammetry is very well defined, and consistent with the formation of an ionic liquid; the resulting oxidative product is an oily material. We have previously shown that the more hydrophobic anions (such as ClO_4^- or AsF_6^-) insert at more negative potentials.[8,9,17] Furthermore, there is a Nernstian dependence of the midpoint potential on the anion concentration in the supporting electrolyte (60 mV per decade), as implied by process A.[8,12b]

3.2.1 Further Evidence for Insertion at the Three Phase Boundary. In the above discussion, and in previous papers,[8,12b] we have suggested that the insertion of the anions takes place at the three phase junction of electrode|oil|electrolyte. (It should be noted that in the work of a similar nature undertaken by Scholz,[33−35] insertion in this manner has been *assumed*, based on the electrical insulating properties of the oily deposit.[37]) Two new experiments confirm this type of behavior. First, an electrode is fully coated with a thin film of electroactive oil and subsequently immersed into aqueous electrolyte (at neutral pH[9,15]). This was undertaken for the case of a gold ring electrode (of dimensions reported in the Experimental) modified with a THPD film, so that no Au was exposed, and immersed into a 0.1 M aqueous solution of sodium perchlorate, see Figure 5a. Figure 5c illustrates the observed voltammetry. We note that the current|voltage behavior is purely resistive, corresponding to ohmic drop across the liquid|liquid interface. Interestingly, the resistance of the oil film changes from ca. 800 MΩ on the first scan to approximately 160 MΩ on the fifth scan. This was not observed when the ring electrode was fully coated with *n*-hexane instead of THPD, suggesting that this effect is consistent with the partitioning of water or electrolyte into the film. In contrast, when a part of the ring electrode is exposed to both aqueous electrolyte solution (0.1 M NaSCN) and THPD (by, for example, hollowing out the inner insulation of the ring electrode, and depositing a small droplet of THPD in this "dip", Figure 5b), the voltammetry that has been previously seen[8−17] for the case of microdroplets of THPD immobilized on a rough electrode surface (bppg), is observed, as indicated in Figure 5d (E_{mid} = 0.11 V vs SCE, consistent with the results obtained at a basal plane pyrolytic graphite electrode[8,9]). Additional confirmation that the reaction occurs at this well-defined triple phase boundary can be seen from photographic images of the THPD deposit oxidized in 0.1 M NaSCN aqueous solution by potentiostating at 0.4 V vs SCE for 30 s, depicted in Figure 5e.

In the second experiment, we emulsify THPD with an aqueous electrolyte solution known to induce case (i) type insertion (e.g., sodium thiocyanate). We have previously shown that the application of power ultrasound to a liquid/liquid interface results in an intra muros emulsion.[32,38] These media are well suited for biphasic electrochemical experiments, since they are highly conductive.[32] Furthermore, since the emulsion consists of small droplets of THPD dispersed into the aqueous solution, electron transfer between the electrode and the electroactive oil can only occur at the three-phase junction

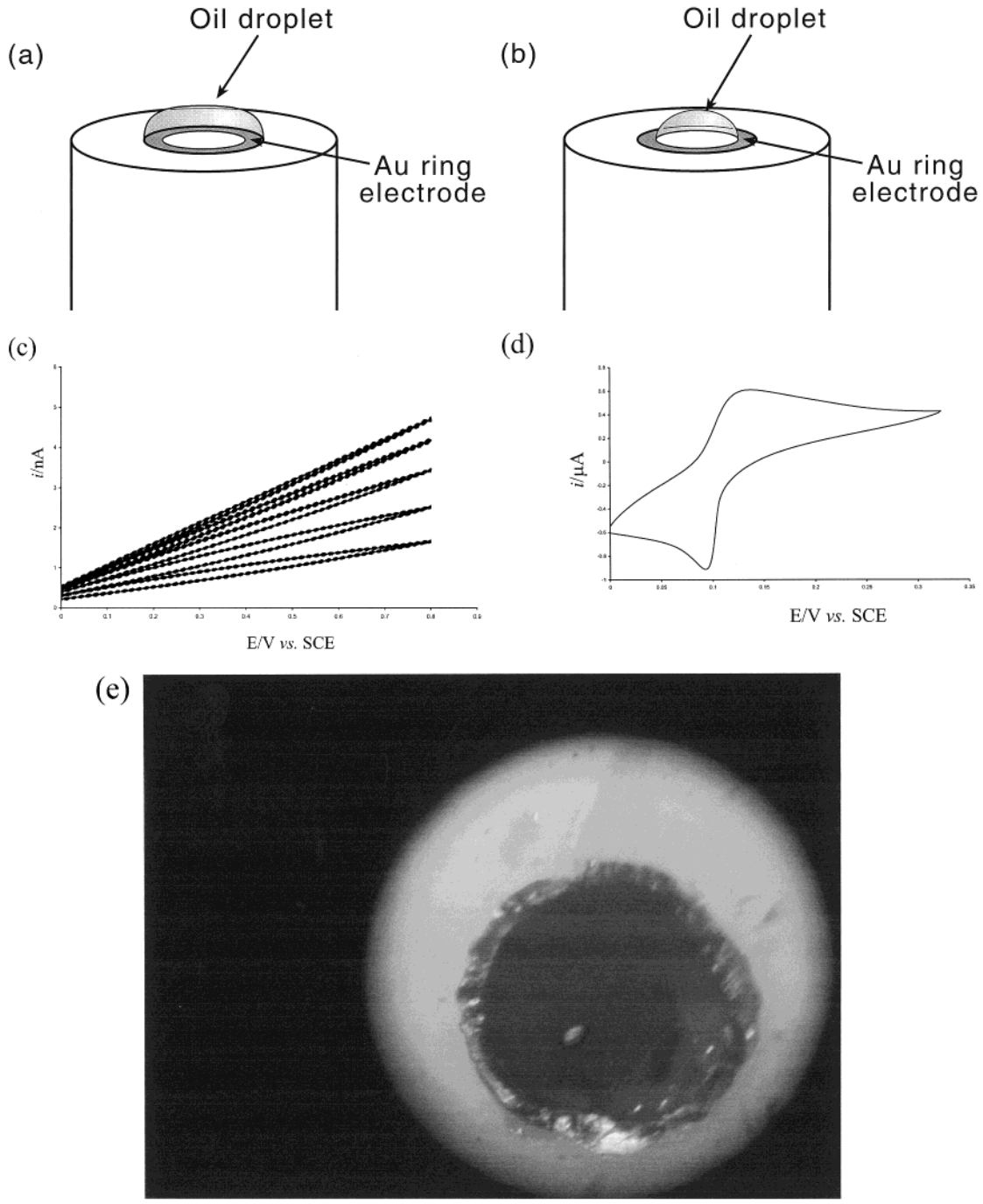

Figure 5. (a) Schematic illustration of a ring electrode fully coated with a TRPD film. (b) Schematic illustration of a TRPD-modified electrode exhibiting a well-defined triple phase junction. (c) Voltammetry at an electrode prepared as in (a). (d) Voltammetry of an electrode prepared as in (b) immersed in 0.1 M sodium perchlorate solution (voltage sweep rate is 100 mV s^{-1}). (e) A photographic image of the electrode surface as in (b) and (d), immediately after the first oxidative scan. The dark region close to the inner ring perimeter indicates that the oxidative voltammetry (to form a species related to Würster's Blue), takes place at the three phase junction.

formed when the oil microdroplet is forced to come into contact with the electrode surface. Accordingly, a quantity of THPD (1.7 g, 3.8 mmol) was placed on top of a 0.1 M solution of sodium thiocyanate (12 cm^3).[39] These liquids were emulsified using 20 kHz power ultrasound at various intensities, and the corresponding current|voltage behavior recorded both under insonation and in quiescent solutions immediately after the acoustic emulsification process had taken place. Figure 6 illustrates typical voltammograms. The use of ultrasound intensities of 215 W cm^{-2} has a substantial effect upon the shape of the voltammetric signal (Figure 6a): first, there is a large amount of noise superimposed upon the signal, consistent with the turbulent mass transport regime and the effects of cavitation at the liquid/liquid interface. Second, on the reverse reductive sweep of the potential, there is a peak in the wave, irrespective of the ultrasonic intensity ($190 < I/W\ cm^2 < 250$). This is strong evidence for the presence of THPD droplets attached to the electrode surface, which are not removed by cavitational processes taking place at the electrode surface. Due to the fast material transport regime present in this system, it is likely that a large fraction of the electroactive oil is immobilized on the electrode in this manner. It is likely that the primary reason for the build up of THPD upon the electrode surface is due to it "wetting" the electrode surface better than the aqueous solution.

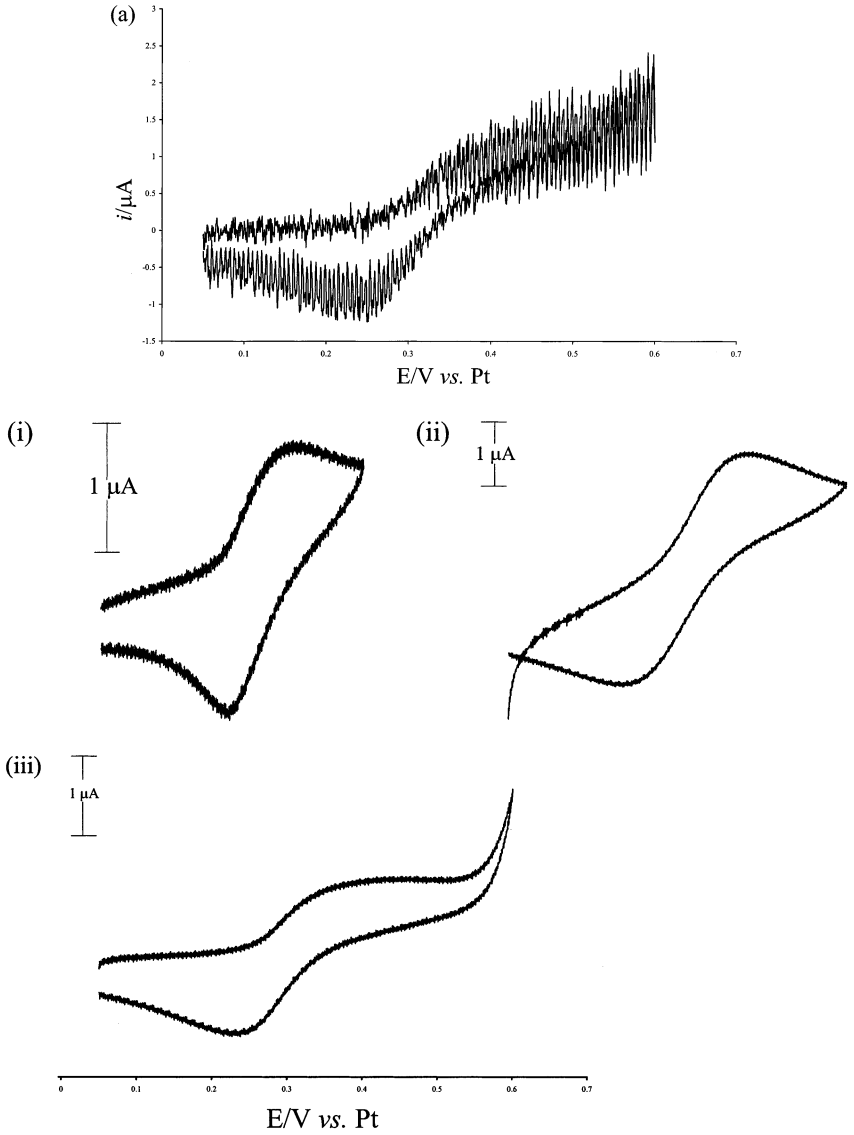

Figure 6. (a) Sonovoltammogram recorded at a scan rate of 100 mV s^{-1} illustrating the electrochemistry of a 1.7 g THPD/0.1 M NaSCN aqueous biphasic emulsion. The ultrasound intensity was 215 W cm^{-2}. (b) The voltammetry of the THPD/SCN^- biphasic emuslion system after insonation emulsion for various time periods at 215 W cm^{-2}; (i) one, (ii) two, (iii) six min of ultrasonic irradiation.

Figure 6b shows quiescent voltammograms corresponding to oxidation of the sono-deposited THPD droplets in the presence of 0.1 M sodium thiocyanate, after insonation using 215 W cm^{-2} for various time periods. It can be seen that increasing the time period between electrochemical runs initially causes an increase in the voltammetric signal, consistent with the greater deposition of THPD onto the electrode surface. Further increases in the sonication times then causes the *opposite* effect; the voltammetric signal *diminishes*. This general effect of a maximum in the observed voltammetric peak current has been observed in similar cases,[12b,13] and has been explained on the basis of conflicting trends. Acoustic streaming processes induced by ultrasound encourage the deposition of THPD onto the electrode surface. However, for the electrochemical process (anion insertion upon THPD oxidation) to take place, there is a space requirement since *the electrochemistry takes place at the three-phase junction*. As the acoustic streaming process deposits increasing quantities of THPD onto the electrode surface, there is less space for electron-transfer to take place at the triple-phase boundary, resulting in a decrease in the voltammetric signal, as the net amount of drop "edge" is decreased. This form of modification of the electrode surface clearly has implications in the field of sono-emulsion electrochemistry.[32,38]

Having thus presented further strong evidence for insertion process taking place at the electrode|oil|electrolyte triple phase junction, we turn to the voltammetric characteristics of the four electroactive oils in the presence of a variety of aqueous electrolyte solutions.

3.2.2 Electrogeneration of Novel Ionic Liquids. Figure 7 illustrates the first oxidation of the electroactive oils TRPD (R = *n*-butyl, *n*-hexyl, *n*-heptyl, and *n*-nonyl) in the presence of perchlorate, hexafluorophosphate and hexafluoroarsenate anions, in aqueous solution at neutral pH, and with ionic strength of 0.1 M. In Figure 8, the voltammetry shows the insertion of the halide ions, Cl^-, Br^-, and I^-. The voltammogams in these figures suggest that we can divide anions that insert into the TRPD droplets into two distinct categories. The first category (type α) is identified by stable one-electron oxidation and reduction signals; the anion species that inserts to generate the ionic liquid is also expelled from the oily deposits upon rereduction of the $TRPD^{+\bullet}$ radical cation

$$\mathrm{TRPD(oil)} + \mathrm{X^-(aq)} - \mathrm{e^-} \rightarrow [\mathrm{TRPD^{+\bullet}X^-}](\mathrm{oil}) \quad \text{(D)}$$

$$[\mathrm{TRPD^{+\bullet}X^-}](\mathrm{oil}) + \mathrm{e^-} \rightarrow \mathrm{TRPD(oil)} + \mathrm{X^-(aq)} \quad \text{(E)}$$

The presence of multiple peaks upon rereduction of the $TRPD^{+\bullet}$

TABLE 1: Categorization of the Immobilized Voltammetry of N,N,N′,N′-Tetraalkyl-*para*-phenylenediamine (TRPD, R = *n*-butyl, *n*-hexyl, *n*-heptyl, *n*-nonyl) in the Presence of Various Aqueous Electrolytes[a]

anion[a]\oil	TBPD	THPD	THePD	TNPD
AsF_6^-	i[b,c]	i	i	i
PF_6^-	i[b,c]	i	i	i
ClO_4^-	i	i	i	i
NO_3^-	ii	i	i	i
IO_3^-	ii	ii	ii	ii
SCN^-	ii	i	i	i
OCN^-	ii	ii	ii	ii
F^-	ii	iii	ii	ii
Cl^-	ii	ii[c]	i[c]	i[c]
Br^-	ii	i[c]	i[c]	i[c]
I^-	ii[c]	i[c]	i[c]	i[c]
N_3^-	ii	iii	iii	iii
OAc^-	ii	iii	ii	ii
SO_4^{2-}	ii	iii	ii	ii
Tartrate	ii	ii	ii	ii
Oxalate	ii	ii	ii	ii

[a] Because TRPD's are oxidized to the respective $TRPD^{+\bullet}$ radical cations, the electroneutrality principle holds that the counterion must be negatively charged. It is for this reason that we consider only anions in the aqueous phase. [b] Slight loss of siganl ($\ll 5\%$) occurs over several cycles. [c] Multiple back peaks present in the range 10−100 mV s^{-1}.

moiety, while there is only one stable and narrow oxidative peak is characteristic of the second type of voltammogram (type β). In Table 2, we have divided up the various ions according to their voltammetric behavior. In this Table type α behavior is easily understood by reference to processes D and E. Type β characteristics have been explored in a previous paper.[11] For the case of the chloride and bromide ions, Figure 8, parts a and b, shows that there are in fact two back peaks associated with the rereduction of the $TRPD^{+\bullet}$ radical cation. As reported earlier,[11] heating the electrochemical cell to 40 °C (or higher) causes the second response to disappear, leaving only the first response as fully reversible. This can interpreted in terms of an ECE-type scheme, in which the second electrochemical step takes place upon reversal of the potential sweep

$$\mathrm{TRPD(oil)} + \mathrm{X^-(aq)} - \mathrm{e^-} \rightleftarrows [\mathrm{TRPD^{+\bullet}X^-}](\mathrm{oil,A}) \quad \text{(F)}$$

$$[\mathrm{TRPD^{+\bullet}X^-}](\mathrm{oil,A}) \rightleftarrows [\mathrm{TRPD^{+\bullet}X^-}](\mathrm{oil,B}) \quad \text{(G)}$$

$$[\mathrm{TRPD^{+\bullet}X^-}](\mathrm{oil,B}) + \mathrm{e^-} \rightleftarrows \mathrm{TRPD(oil)} + \mathrm{X^-(aq)} \quad \text{(H)}$$

In the above processes, A is the state of the initial liquid, and B represents a higher energy modification.[11] Although this structural change can be due to a phase transition process, this was ruled out on the basis that this is inconsistent with observations made on the type α systems.[11] It was suggested that due to the greater solvation of these types of anions when compared to the generally bigger type α anions, it is likely that water rapidly co-inserts with the anion; the direct insertion of the halide ion not being possible due to the presence of a kinetic barrier.[11]

The case of the insertion of the iodide anion is subtly different to the behavior described above, in that there is a very large separation between the oxidation and rereduction peak potentials, see Figure 8c. Integration of the current|voltage behavior allows the deduction of the charge passed. At scan rates of 20 mV s^{-1}, and less, this process gives a result of 2.25×10^{-4} C for oxidation of 1.3 nmol of THPD. This is approximately twice that seen for a one-electron conversion,[40] and is indicative of a redox catalytic process mediated by the $TRPD^{+\bullet}$ radical cation.[41−43] Although there is only one oxidation peak (labeled P_1), experiments undertaken at a variety of scan rates, Figure 8c(i), (ii), and (iii), shows that there are up to three back peaks (at the faster scan rates), which may be labeled as P_1', P_2', and P_3'. From comparison with the voltammograms in Figure 8, parts a and b (for the case of oxidation in chloride or bromide-based supporting electrolytes), we may attribute P_1' to correspond to the expulsion of solvated I^-, P_2' to be expulsion of nonsolvated I^-, and P_3' to be the expulsion of anionic redox catalytic products. Again, we note that the chemical step corresponding to the transition of phase A to phase B (step G) takes place much faster in the case of the more hydrophobic iodide case than for Cl^- or Br^-. We suggest the oxidation takes place via the following mechanism

$$3\mathrm{TRPD(oil)} + 3\mathrm{I^-(aq)} - 3\mathrm{e^-} \rightleftarrows 3[\mathrm{TRPD^{+\bullet}I^-}](\mathrm{oil}) \quad \text{(I)}$$

$$[\mathrm{TRPD^{+\bullet}I^-}](\mathrm{oil}) \rightleftarrows \mathrm{TRPD(oil)} + {}^1/_2\mathrm{I_2(oil)} \quad \text{(J)}$$

$$\mathrm{I_2(oil)} + [\mathrm{TRPD^{+\bullet}I^-}](\mathrm{oil}) \rightleftarrows [\mathrm{TRPD^{+\bullet}I_3^-}](\mathrm{oil}) \quad \text{(K)}$$

$$\text{Overall: } \mathrm{TRPD(oil)} + 3\mathrm{I^-(aq)} - 3\mathrm{e^-} \rightleftarrows [\mathrm{TRPD^{+\bullet}I_3^-}](\mathrm{oil}) \quad \text{(L)}$$

Thus, for full conversion, we observe a three-electron oxidation per TRPD molecule. The fact that we only get, at most, two electrons per TRPD molecule, suggests that the formation of the I_3^- species is in part rate determining. The wide peak-to-peak separation then becomes obvious: it is the I_3^- moiety that is expelled upon rereduction. The Gibbs energy of transfer of tri-iodide from an organic phase to an aqueous phase is generally more favorable than that for iodide,[44] and because the material likely remains a liquid after the first scan, this transfer (expulsion) takes place at more negative potentials than the insertion. We do not observe the insertion of I_3^- immediately after its expulsion, since I_3^- dissociates into I^- and I_2 in the aqueous phase upon expulsion from the oil droplets. As an aside, we note that the above mechanism relies on redox behavior of the I^-/I_2 couple; the oxidation of aqueous iodide to iodine takes place at 0.5 V vs SCE on basal plane pyrolytic graphite electrode materials.[45] As this couple is more negative (the oxidation takes place more easily) than those for Br^-/Br_2 and Cl^-/Cl_2, such a mechanism is unlikely to be operative in the case of the electroinsertion of Br^- and Cl^- into the TRPD oil deposits.

The cases of hexafluorophosphate and hexafluoroarsenate insertion via the electrochemical oxidaton of droplets of N,N,N′,N′-tetrabutyl-*para*-phenylenediamine at neutral pH are illustrated in Figures 7b and c. Although the voltammetric profiles in the presence of PF_6^- and AsF_6^- are reproducible upon multiple scans, and of type α in the case of the higher homologues, they are type β for TBPD. As in the case for bromide insertion into the oil deposits, we observe a single one-electron oxidation peak (P_1), and two reverse peaks, one corresponding to the reverse of P_1 (P_1')and another, P_2'. A scan rate dependence of the voltammetry indicated that at faster scan rates (100 mV s^{-1}), P_2' virtually disappears, it being almost entirely replaced by P_1'. This is indicative of the ECE-type mechanism proposed above. To understand further this unusual behavior, a variable temperature study was undertaken (in the range $2 < T/°C < 60$). As in the case of bromide insertion, increasing temperature caused P_2' to diminish, even at the slowest scan rates (5 mV s^{-1}). This type of behavior is indicative of a favorable chemical process associated with a reduction of entropy ($\Delta G° < 0$, $\Delta S° < 0$). A variable anion concentration study further revealed a Nernstian dependence of E_{mid} for processes P_1 and P_1', hinting that this behavior is due to a

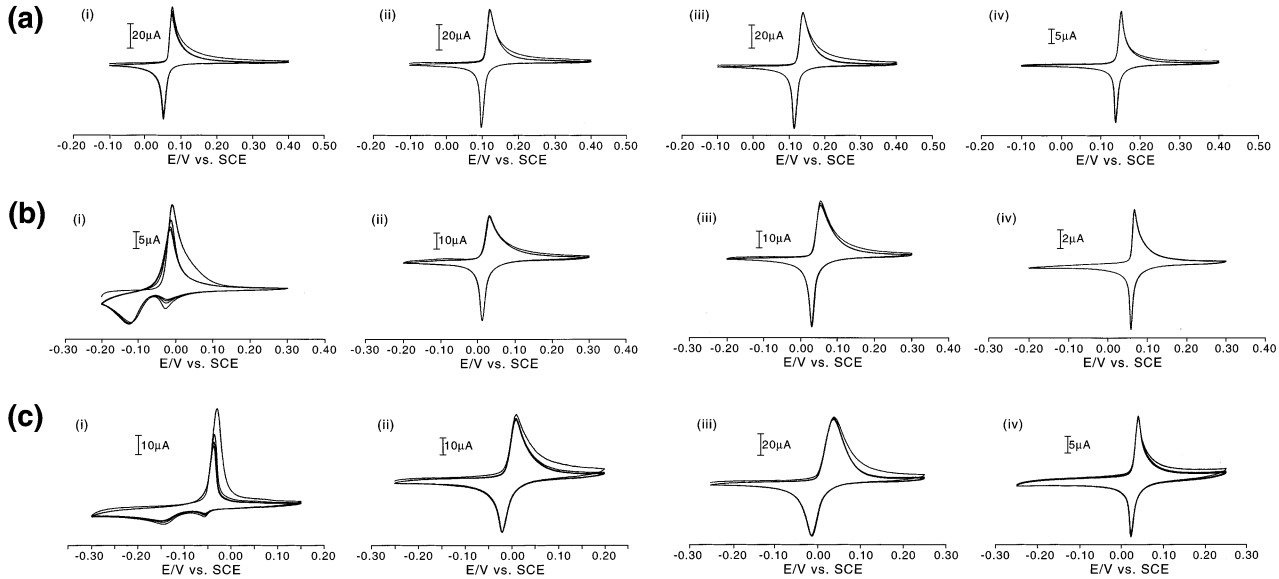

Figure 7. The current/voltage behavior (at 10 mV s^{-1}) of the bppg-immobilized TRPD's ((i) TBPD, (ii) THPD, (iii) THePD, and (iv) TNPD) with anions that have case (i) characteristics. (a) 4 nmol TRPD with 0.1 M aqueous perchlorate, (b) 4 nmol TRPD with aqueous 0.1 M hexafluorophosphate, and (c) 4 nmol TRPD with 0.1 M aqueous hexafluoroarsenate (at neutral pH).

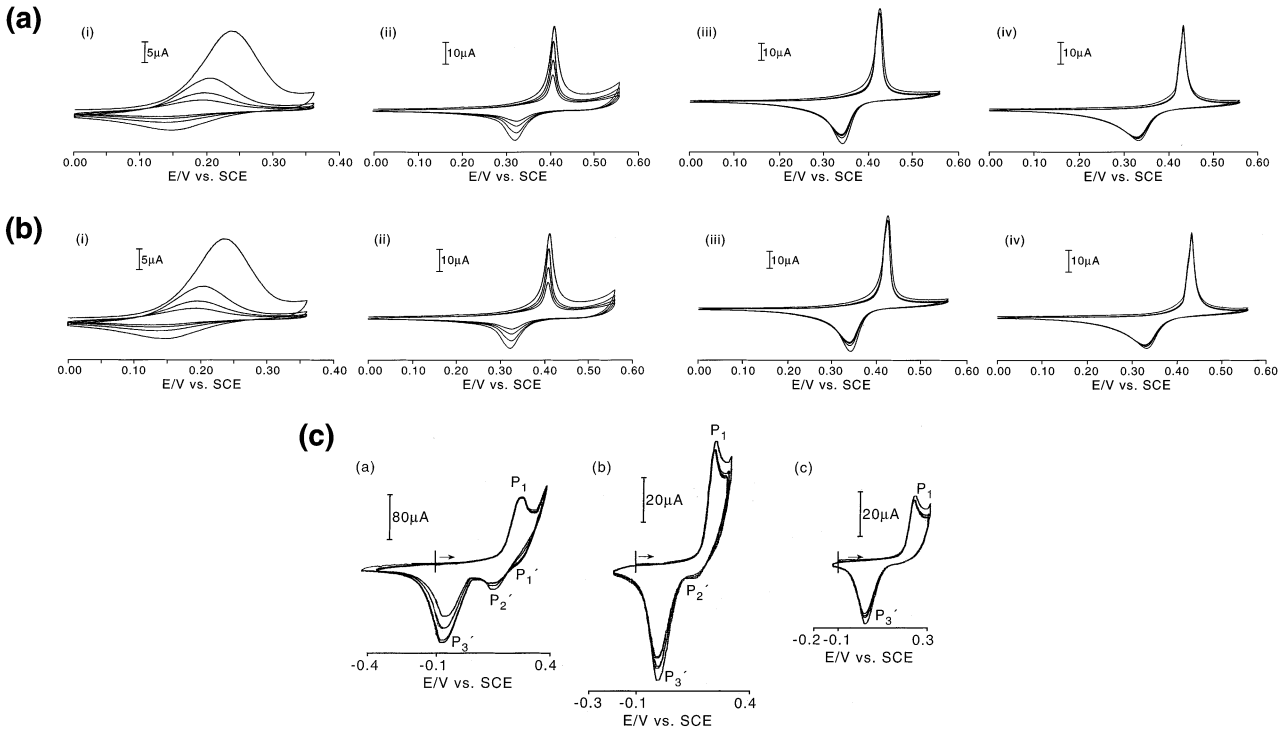

Figure 8. The voltammetry of the TRPD species in the presence of 0.1 M aqueous halide ions at a 4.9 mm diameter bppg electrode. (a) 4 nmol TRPD with Cl^- (scan rate is 10 mV s^{-1}, (i) TBPD, (ii) THPD, (iii) THePD, and (iv) TNPD). (b) 4 nmol TRPD with Br^- (scan rate is 10 mV s^{-1}, (i) TBPD, (ii) THPD, (iii) THePD and (iv) TNPD). (c) 1 nmol THPD with I^-, at scan rate of (a) 100, (b) 20, and (c) 10 mV s^{-1}.

chemical process taking place in the oil droplets, rather than in the solution. In addition, the process responsible for P_2' appears to be more dominant in the case of low solution concentrations of PF_6^-. The complexity of this voltammetry is further compounded by the very hydrophobic nature of these anions (with quoted Gibbs energies for transfer from water to nitrobenzene as 7.2 and −42 kJ mol^- for PF_6^- and AsF_6^- respectively).[17] Furthermore, Maldi TOF mass spectrometric analysis of the oil deposits after electrooxidation of TBPD droplets in the presence of PF_6^- ions revealed spectra corresponding to the $TBPD^{+\bullet}$ cation radical, its breakdown, and matrix fragments. We suggest that the chemical step in the ECE mechanism outlined by processes F − H is probably due to the formation of a tight ion pair of PF_6^- or AsF_6^- with the $TBPD^{+\bullet}$ cation radical. Ion pairing effects are well-known to participate in electrochemical processes,[46] and also in ionic fluids.[47] This pathway is more likely to take place for these anions than in the case of the halide ions, since their larger size reduces their charge density, causing them to be less solvated in the lipophobic aqueous phase. At present we may only speculate on the reason we only observe this type of behavior with the tetrabutyl derivative; it is possible that this is due to charge screening effects by the alkyl chains in the $TRPD^{+\bullet}$ species.

The electrogeneration of stable ionic liquids resulting from the first oxidation of TRPD microdroplets immobilized on a basal plane pyroltic graphite electrode has been shown to take

TABLE 2: Classification of the Electrochemically generated Ionic Liquids into Types α and *β* Depending upon Their Voltammetric Features (see text and Figures 7 and 8)

anion\oil	TBPD	THPD	THePD	TNPD
AsF_6^-	*β*	α	α	α
PF_6^-	*β*	α	α	α
ClO_4^-	α	α	α	α
SCN^-	n/a	α	α	α
NO_3^-	n/a	α	α	α
Cl^-	n/a	n/a	*β*	*β*
Br^-	n/a	*β*	*β*	*β*
I^-	n/a	*β*	*β*	*β*

place at the three phase boundary. Furthermore, we have seen that voltammetric nuances can be explained in terms of the rapid co-insertion of solvent molecules with the anion, redox catalysis, or the formation of tight ion pairs within the ionic liquid. We next turn our attention to the case where the voltammetric waves are unstable and indicative of material loss from the electrode surface.

3.3 Case (ii): Electrochemically-Induced Ion Expulsion Processes. This section investigates the processes responsible for the voltammetric features indicated in Figure 4(ii), viz. narrow oxidative and reduction peaks, albeit with successively decreasing peak heights upon redox cycling. Such voltammeric behavior has been documented for the case of the oxidation of microdroplets of N,N,N′-trihexyl-*para*-phenylenediamine (Tri-HPD) in the presence of a 0.1 M solution of sodium perchlorate,[9] and for the oxidation of electrode-immobilized droplets of decane containing N,N,N′,N′-tetramethyl-*para*-phenylenediamine in the presence of 0.1 M aqueous sodium perchlorate.[48] The use of an electrochemical quartz-crystal microbalance in the former study was employed to show that such voltammetric behavior occurs with concomitant loss of material from the electrode surface; the oil dissolves. In a recent paper,[17] based upon the seemingly one-electron nature of this process, we have suggested that associated electrochemical process is

$$\mathrm{TRPD(oil)} - \mathrm{e}^- \rightleftarrows \mathrm{TRPD}^{+\bullet}\mathrm{(aq)} \qquad \text{(M)}$$

This process takes place since the transfer energy of the anion from the organic to the aqueous phase is very large, making its insertion into the electroactive oil deposit thermodynamically unfavorable.[17] Thus, the transfer of the $TRPD^{+\bullet}$ radical cation into the solution takes place, *without the formation of an ionic liquid*.[17] From Table 1, it is clear that this kind of behavior is observed for small anions that are strongly solvated in the aqueous phase, like, for example, fluoride and sulfate ($\Delta G_{tr}^{w\rightarrow nb} > 40$ kJ mol^{-1}).[44] Although it would be expected that the Gibbs energy for the transfer of the tetraalkyl-*para*-phenylenediamine radical cation become less favorable with increasing hydrophobicity (viz., increasing substitution),[17] it is evident (from Table 1) that even the radical cation derived from the tetranonyl species may be transferred across the liquid|liquid interface.

If the process responsible for type (ii) behavior is the dissolution of the $TRPD^{+\bullet}$ radical cation, as suggested above, it might take place either at the liquid/liquid interface, as in the case of ferrocinium ion transfer across the area of the nitrobenzene-microdroplet|water interface in the work described by Nakatani,[49] or at the triple phase boundary. Further, although the above dissolutive process appears to be conceivable, it does not fully rule out the possibility of a reaction between the $TRPD^{+\bullet}$ radical cation and the electrolytic anion at the triple phase boundary taking place to yield electrochemically inactive products. Although the EQCM experiments suggest that this is unlikely to take place (because a reaction is likely to increase the mass, unless it proceeds with a volume change),[15] we nevertheless still consider this as a viable pathway. To distinguish between these possible pathways, we consider each of the mechanisms in turn, and focus upon the kinetics of the process. In all cases the random array of droplets is approximated by a single hemispherical droplet of fixed size. In so doing, we assume that the microdroplets have a diffusional independence.

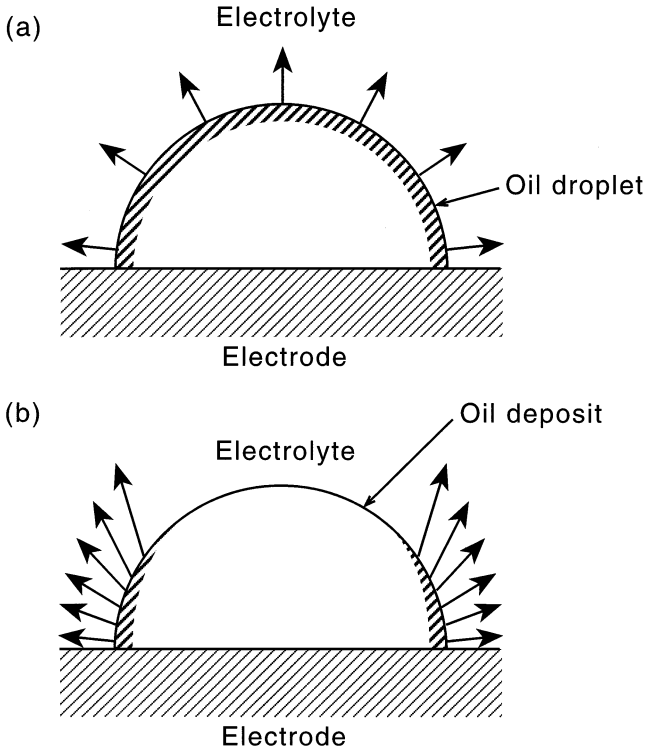

Figure 9. Schematic representation of the dissolution process: (a) ion expulsion from the liquid|liquid interface (model b); (b) ion expulsion from the three-phase boundary (model c).

3.3.1 Dissolution at the Liquid|Liquid Interface. We consider the electrochemical process taking place in accordance with model b, but with the expulsion of the $TRPD^{+\bullet}$ radical cation, see Figure 9a. The amount of material diffusing from the electrode surface per unit time (j/mol s^{-1}) from the surface of the oil droplets will be proportional to the surface area of the droplet

$$j = k \times 2\pi r^2 \qquad (1)$$

where r is the radius of the droplet, and the proportionality constant, k, represents the rate constant for dissolution (in units of mol cm^{-2} s^{-1}). Hence, the rate of dissolution is given by

$$\frac{dn}{dt} = -2k\pi r^2 \qquad (2)$$

where n refers to the number of moles of TRPD oxidized at the electrode surface, given by the following expression, assuming all TRPD molecules in the oil droplet are oxidized

$$n = \frac{2}{3}\pi r^3 \frac{\rho}{M_r} \qquad (3)$$

in which ρ represents the density of the TRPD oil, and M_r its molecular mass. Rearranging eq 3 in terms of r and substituting this into eq 2 yields

$$\frac{dn}{dt} = -k\sqrt[3]{\frac{18\pi n^2 M_r^2}{\rho^2}} = -k_{eff}\sqrt[3]{n^2} \quad (4)$$

in which the apparent two-thirds order rate constant k_{eff} is given by

$$k_{eff} = k\sqrt[3]{\frac{18\pi M_r^2}{\rho^2}} \quad (5)$$

Integration of the first-order differential equation (equation 4) under the pertinent boundary conditions, gives

$$3(\sqrt[3]{n_0} - \sqrt[3]{n}) = k_{eff}t \quad (6)$$

In this equation, n_0 is the initial number of moles of TRPD deposited upon the electrode surface. Equation 6 can be expressed more succinctly for the experimental purposes in terms of the charge transferred (Q)

$$\sqrt[3]{Q} = \sqrt[3]{Q_0} - \frac{k_{eff}\sqrt[3]{F}}{3}t \quad (7)$$

F is the Faraday constant (96 485 C mol^{-1}), and Q_0 is the charge required to oxidize all the TRPD into the cation radical on the first oxidative scan. This equation predicts that the cube root of the integrated charge should be a linear function of time if the proposed mechanism is appropriate.

3.3.2 Dissolution at the Electrode|Oil|Electrolyte Triple Phase Junction. In a manner similar to model c for electrochemically induced anion insertion process (see Figure 9b), we consider the expulsion of the electrogenerated radical cation to be initiated at the contact line of the three phases oil, electrode and electrolyte. The only points of contact between all three phases is the base of the hemispherical droplet; the locus of the triple phase junction thus traces out a circle. As before, we may write

$$j = k \times 2\pi r \quad (8)$$

Hence, the rate of dissolution can be written as

$$\frac{dn}{dt} = -k'_{eff}\sqrt[3]{n} \quad (9)$$

in which the one-third-order effective rate constant, k'_{eff}, is given by

$$k'_{eff} = k\sqrt[3]{\frac{12\pi^2 M_r}{\rho}} \quad (10)$$

Integration under the appropriate boundary conditions (vide supra) yields

$$\frac{3}{2}(\sqrt[3]{n_0^2} - \sqrt[3]{n^2}) = k'_{eff}t \quad (11)$$

which can be expressed more succinctly as

$$\sqrt[3]{Q^2} = \sqrt[3]{Q_0^2} - \frac{2}{3}k'_{eff}\sqrt[3]{F^2}t \quad (12)$$

Thus, for the dissolution kinetics to follow this model, there will be a linear dependence on time of the cube root of the squared integrated charge.

3.3.3 Reaction of Inserted Ions. The rate of reaction between the radical cation and the electrochemically inserted anion is given by

$$\frac{dn}{dt} = -kn[X^-] \quad (13)$$

where $[X^-]$ refers to the concentration of the inserted ion. In writing eq 13, we assume the droplet effectively behaves as a "thin layer cell", so that diffusional processes are fast compared with the reaction chemistry. Equation 13 also applies to other models. To satisfy the electroneutrality principle, $n = [X^-]$. Thus

$$\frac{1}{n} - \frac{1}{n_0} = kt \quad (14)$$

or alternatively

$$Q = \frac{Q_0 F}{Q_0 kt + F} \quad (15)$$

Hence, the inverse integrated charge will be linearly dependent upon time, characteristic of second-order kinetic processes.

3.3.4 Assessment of the Three Kinetic Models in Respect of the Experimental Data. Analysis of all voltammograms exhibiting case (ii) characteristics was undertaken by plotting the appropriate graph for all three types of mechanism, for scan rates in the range $10 < \upsilon/\text{mV s}^{-1} < 500$. Figure 10 illustrates a selection of such plots, in which the appropriate charge function under the oxidations scans is plotted against the total time taken to scan until the end of the oxidation scan, for each scan during consecutive cycling. The plots corresponding to the two-thirds-order dissolution pathway at the liquid/liquid interface are in all cases rigorously linear, whereas those for the one-third order dissolution at the three-phase boundary in all cases, or that postulated for the second-order reactive mechanism are appreciably curved, suggesting the veracity of process M, and that cation expulsion takes place via model b rather than c. For this to occur, we infer fast charge transfer over the liquid|liquid interface, possibly in the form of the surface diffusion of TRPD$^{+\bullet}$-anion pairs.

Experimental values for $k_{eff}/\text{mol}^{1/3}\ \text{s}^{-1}$ can be deduced from the gradients of the plots based upon eq 7 depicted in Figure 10 for each scan rate. These are summarized in Table 3; k_{eff} is more or less independent of the nature of the oil and of the solution-phase anionic species, with an average value of 6.8×10^{-6} mol$^{1/3}$ s^{-1}. The average k_{eff} value for each electroactive oil is seen to decrease with oil hydrophobicity: the *n*-butyl derivative appears to undergo electrochemically induced cation radical expulsion in the presence of anions (such as SCN$^-$ or NO$_3^-$) that in the presence of the other more hydrophobic oils yield stable voltammetric signals upon consecutive potential sweeps. This is consistent with the smaller Gibbs energy of transfer of for the TBPD$^{+\bullet}$ cation radical from nitrobenzene to water, than THPD$^{+\bullet}$, or higher homologues.[17] Furthermore, the *n*-nonyl species is observed to be the most hydrophobic, consistent with the observation that the E_{mid} values for this species are more negative than for the others.[17] Following Scholz,[35] if we take the number of carbon atoms in the side chain (N_C) as a measure of the hydrophobicity, we may apply a nonlinear least-squares analysis of the average k_{eff} data, and deduce

$$k_{eff}^{av.} = 2.25 \times 10^{-5} - 8.6 \times 10^{-6}\ln(N_C); R^2 = 0.96 \quad (16)$$

It should be noted that a peculiarity is observed in the absolute k_{eff} values on comparison of Table 1 with Table 3: with certain

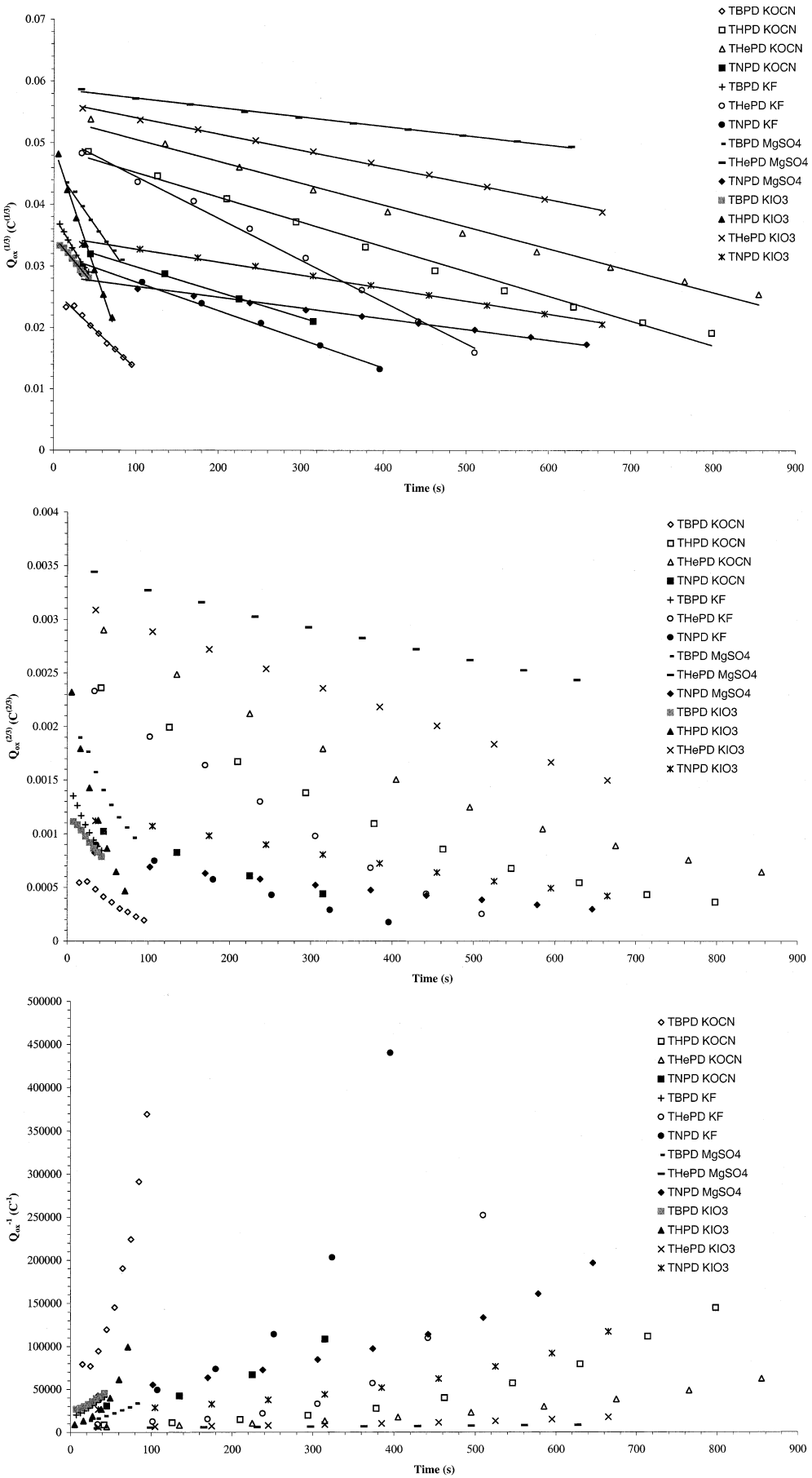

Figure 10. Typical plots showing the analysis of the experimental data via the three kinetic models: (a) dissolution at the liquid|liquid interface, (b) cation expulsion at the triple phase junction, and (c) chemical reaction of ions. All three plots examine 4 nmol TRPD with OCN^-, IO_3^-, F^- and SO_4^{2-} (at a concentration of 0.1 M in the aqueous phase).

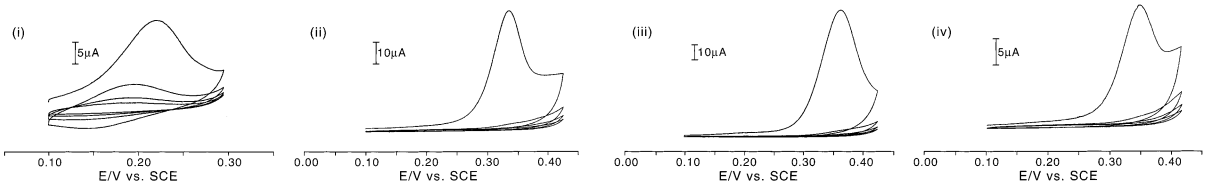

Figure 11. Cyclic voltammograms showing the voltammetry (at 10 mV s^{-1}) 4 nmol TRPD immobilized as microdroplets on a 4.9 mm basal plane pyrolytic graphite electrode an immersed into 0.1 M aqueous sodium azide solution. (a) R = *n*-butyl, (b) R = *n*-hexyl, (c) R = *n*-heptyl, and (d) R = *n*-nonyl.

TABLE 3: Values of k_{eff}/mol$^{1/3}$ s^{-1} Based upon Cation Expulsion from the Liquid|Liquid Interface (model b), Case (ii) Behavior (see text and Figures 9 and 10)

anion\oil	TBPD	THPD	THePD	TNPD
NO_3^-	1.9×10^{-5}	n/a	n/a	n/a
SCN^-	1.3×10^{-6}	n/a	n/a	n/a
OCN^-	7.8×10^{-6}	2.6×10^{-6}	2.3×10^{-6}	2.7×10^{-6}
OAc^-	1.1×10^{-5}	n/a	4.2×10^{-6}	3.4×10^{-6}
IO_3^-	1.2×10^{-5}	2.6×10^{-6}	1.7×10^{-6}	1.4×10^{-6}
N_3^-	7.4×10^{-6}	n/a	n/a	n/a
I^-	3.1×10^{-7}	n/a	n/a	n/a
Br^-	1.4×10^{-5}	n/a	n/a	n/a
Cl^-	1.0×10^{-5}	5.4×10^{-7}	n/a	n/a
F^-	1.5×10^{-5}	n/a	4.4×10^{-6}	3.1×10^{-6}
SO_4^{2-}	1.2×10^{-5}	n/a	1.0×10^{-6}	1.2×10^{-6}
Tartrate	1.2×10^{-5}	7.9×10^{-6}	7.7×10^{-6}	5.4×10^{-6}
Oxalate	1.4×10^{-5}	1.6×10^{-5}	8.2×10^{-6}	6.2×10^{-6}
Average	1.0×10^{-5}	5.9×10^{-6}	4.2×10^{-6}	3.3×10^{-6}

anions (for example sulfate, acetate, and fluoride) the hexyl derivative, THPD, appears to exhibit quasi-case (iii) type behavior, whereas both the lower and the higher homologous derivatives behave with case (ii) characteristics. Furthermore, in the presence of chloride supporting electrolytes, THPD shows case (ii) behavior, whereas that for THePD and TNPD is of case (i), type β. Although we may speculate that these effects might be due to unusually fast cation expulsion in the THPD system (based on the data from the higher homologues), as opposed to a reaction taking place with in the oil, the experimental data and our current understanding of the physical chemistry of the microdroplet environment do not yet support enough conclusions for further comment.

To summarize, we have observed that in contrast to the case of electrochemically induced anion insertion, dissolution (cation expulsion) takes place at the liquid|liquid interface, with the initial electron transfer probably taking place at the three phase boundary. It remains to discuss the occurrence of case (iii) voltammetry, which we next address.

3.4 Case (iii): Chemical Reactions at the Electrode|Oil|Electrolyte Triple Phase Junction. As mentioned earlier, the characteristic of the current|voltage behavior for case (iii) systems is a single large oxidation peak, no reverse reduction peak, followed by effectively resistive behavior upon subsequent cycling. These characteristics are consistent with the "passivation" of the modified electrode. Figure 11 illustrates the voltammetric profiles of a system that exhibit this kind of behavior. In this system, the TRPD oil is oxidized in the presence of the azide anion. This system behaves as case (ii) when the electroactive oil is TBPD, probably owing to the preferential formation of aqueous solution-based ion pairs. The voltammetry for the TRPD (R = *n*-hexyl, *n*-heptyl, *n*-nonyl)/azide system is peculiar, in that the first peak is very broad. Integration of the charge passed during the electrochemical process reveals that this is approximately two electrons (1.9 ± 0.5) when employing scan rates of 10 mV s^{-1}. This suggests that the TRPD-azide system follows an intermolecular electron transfer process. We have previously seen this in the case of the TRPD-iodide system (vide supra). There, the whole process was fully reversible, due to the tri-iodide product being anionic. In this case, the electrochemical process is stopped, since the oil-insoluble products form in or on the organic phase *at the site of the electrochemical step*. This has to be at the triple-phase boundary because the azide ion must be uptaken prior to reaction (vide supra). Furthermore, the Gibbs transfer energy for the azide anion from water to nonaqueous solvents is "low" (q.v., §3.3).[50] We have described such phenomena before in the case of a novel photo-Kolbe process, in which $THPD^{+\bullet}$*-sensitized oxidation of the triphenylacetate anion to form insoluble products at the triple phase boundary was observed to cause the signal due to the electrochemical oxidation of THPD in the presence of perchlorate supporting electrolyte to diminish.[13]

A recent paper has reported the reaction between azide anions and arylanthracene radical cations in acetonitrile solutions.[51] On the basis of the easier oxidation of azide in acetonitrile compared with the arylanthracene, it was concluded that the azide anion intramolecularly donates an electron to the radical cation, and in so doing forming $N_3^\bullet$, and ultimately, N_6^-. Although this mechanism may appear plausible in our context, it was observed that azide oxidation of bppg electrodes in aqueous solution does not take place in the range of potentials used to record the voltammograms in Figure 11. To fully understand the nature of the reaction process, THPD deposits that had been oxidized in the presence of azide were analyzed using both Maldi TOF and electrospray mass spectrometry. In both analyses, the major signal was observed at $m/z = 445$, characteristic of the THPD molecule. Other peaks were observed in the Maldi TOF analysis (mainly attributed to the breakdown of the matrix employed), but none arising from N_6^- type intermediates. Following this, electrospray MS measurements were taken, which revealed a major peak at $m/z = 445$ a small peak at $m/z = 486$ and other peaks corresponding to fragments of the THPD molecule. Several peaks around $m/z = 700$ were observed, consistent with the formation of oligomers of fragments in the gas phase. The peak at $m/z = 486$ is not inconsistent with 2-azido-1,4-tetrahexylaminobenzene. Compounds such as these have been isolated by Magnus during the oxidation of TMPD with electrophilic azide reagents.[52] In our case, it may be appreciated that if the inserted azide species nucleophilically attacks the $TRPD^{+\bullet}$ radical cation, $H^\bullet$ is ultimately lost, forming a reduced phenylendiamine species that can easily undergo further oxidation. The byproduct, $H^\bullet$, ultimately will form H^+, which protonates the neutral TRPD species,[9,15] quenching the whole process.

4. Conclusions

The aim of this paper has been to probe the mechanisms responsible for the voltammetry of electroactive oils immobilized in the form of microdroplets on a rough electrode surface. In this paper, we have seen that the microdroplets thus formed are essentially monodisperse, with droplet sizes being

dependent upon the amount of material deposited. Further, we have seen that for anions for which the transfer from aqueous solution into the oil droplet is thermodynamically favorable, electrochemically induced anion insertion takes place at the three phase boundary of electrode|oil|electrolyte. We have shown direct evidence for this process, and in so doing, we have seen how this type of technology can produce ensembles of microrings, and new types of ionic liquid materials. For anions that cannot transfer from the aqueous electrolyte into the oil droplet, cation expulsion takes place at the liquid|liquid-phase boundary, due to fast charge transfer over the microdroplet surface, and with two-thirds-order kinetics. Finally, we have seen that both redox catalysis and that reaction between the ions in such ionic liquid systems is achievable, and that this takes place close to the triple phase junction. The difference between all three "cases" has been illustrated by reference to their particular current|voltage characteristics. It is for this reason that we may categorize anions using the broad descriptors "inserters", "dissolvers", and "reactors", noting that the nature of the countercation plays a significant rôle, as has been observed in the case of the *n*-butyl derivative.

Acknowledgment. We thank the BBSRC and Glaxo-Smit*hkl*ine for providing respectively a studentship and CASE award for S.J.W., and the EPSRC for studentships for C.E.B., R.R.F., and J.D.W. We are grateful to Steve Davies and Steve Bull for providing us with a sample of THPD. Further, we thank Nathan Lawrence, and Frank Marken for helpful discussions regarding aspects of the electrochemistry of phenylenediamines.

References and Notes

(1) See, for example: Welton, T. *Chem. Rev.* **1999**, *99*, 2071.
(2) Earle, M. J.; Seddon, K. R. *Pure Appl. Chem.* **2000**, *72*, 1391.
(3) See for example Every, H.; Bishop, A. G.; Forsythe, M.; MacFarlane, *Electrochim. Acta* **2000**, *45*, 1279.
(4) McEwen, A. B.; Ngo, H. L.; LeCompte, K.; Goldman, J. L. *J. Electrochem. Soc.* **1999**, *146*, 1687.
(5) Gajar, S. A.; Geis, M. W. *J. Electrochem. Soc.* **1992**, *139*, 2833.
(6) Goldman, J. L.; McEwen, A. B. *Electrochem. Solid State Lett.* **1999**, *2*, 501.
(7) Bonhôte, P.; Dias, A. P.; Papageorgiou, N.; Kalyanasundaram, M.; Grätzel, M. *Inorg. Chem.* **1996**, *35*, 1168.
(8) Marken, F.; Webster, R. D.; Bull, S. D.; Davies, S. G., *J. Electroanal. Chem.* **1997**, *437*, 209.
(9) Marken, F.; Compton, R. G.; Goeting, C. H.; Foord, J. S.; Bull, S. D.; Davies, S. G. *Electroanalysis* **1998**, *10*, 821.
(10) Marken, F.; Blythe, A. N.; Compton, R. G.; Bull, S. D.; Davies, S. G. *Chem. Commun.* **1999**, 1823.
(11) Marken, F.; Blythe, A. N.; Wadhawan, J. D.; Compton, R. G.; Bull, S. D.; Aplin, R. T.; Davies, S. G. *J. Solid. State Electrochem.* **2001**, *5*, 17.
(12) (a) Fulian, Q.; Ball, J. C.; Marken, F.; Compton, R. G.; Fisher, A. C. *Electroanalysis* **2000**, *12*, 1012. (b) Ball, J. C.; Marken, F.; Fulian, Q.; Wadhawan, J. D.; Blythe, A. N.; Schröder, U.; Compton, R. G.; Bull, S. D.; Davies, S. G. *Electroanalysis* **2000**, *12*, 1017.
(13) Wadhawan, J. D.; Compton, R. G.; Marken, F.; Bull, S. D.; Davies, S. G. *J. Solid State Electrochem.* **2001**, *5*, 301.
(14) Marken, F.; Compton, R. G.; Goeting, C. H.; Foord, J. S.; Bull, S. D.; Davies, S. G. *J. Solid State Electrochem.* **2001**, *5*, 88.
(15) Schröder, U.; Compton, R. G.; Marken, F.; Bull, S. D.; Davies, S. G.; Gilmour, S. *J. Phys. Chem. B* **2001**, *105*, 1344.
(16) Marken, F.; Hayman, C. M.; Bulman Page, P. C. *Electroanalysis* **2002**, *14*, 172.
(17) Schröder, U.; Wadhawan, J. D.; Evans, R. G.; Compton, R. G.; Wood, B.; Walton, D. J.; France, R. R.; Marken, F.; Bulman Page, P. C.; Hayman, C. M. *J. Phys. Chem. B*, in press.
(18) Scholz, F.; Meyer, B. In *Electroanal. Chem.*; Bard, A. J., Rubinstein, I., Eds.; Vol. 20; Marcel Dekker: New York, 1998.
(19) Monk, P. M. S.; Mortimer, R. J.; Rosseinsky, D. R. *Electrochromism*: *Fundamentals and Applications*; Weinheim-VCH: New York, 1995.
(20) Rosslee, C. A.; Abbott, N. L. *Anal. Chem.* **2001**, *73*, 4808.
(21) Mälkiä, A.; Liljeroth, P.; Kontturi, A.-K.; Kontturi, K. *J. Phys. Chem. B*, **2001**, *105*, 10 884.
(22) Lawrence, N. S.; Davis, J.; Jiang, L.; Jones, T. G. J.; Davies, S. N.; Compton, R. G. *Electroanalysis* **2000**, *12*, 1453.
(23) Lawrence, N. S.; Davis, J.; Jiang, L.; Jones, T. G. J.; Davies, S. N.; Compton, R. G. *Analyst* **2000**, *125*, 661.
(24) Lawrence, N. S.; Davis, J.; Marken F.; Jiang, L.; Jones, T. G. J.; Davies, S. N.; Compton, R. G. *Sens. Acts. B* **2000**, *69*, 189.
(25) Lawrence, N. S.; Davis, J.; Jiang, L.; Jones, T. G. J.; Davies, S. N.; Compton, R. G. *Electroanalysis* **2001**, *13*, 432.
(26) White, P. C.; Lawrence, N. S.; Davis, J.; Compton, R. G. *Anal. Chim. Acta* **2001**, *447*, 1.
(27) Lawrence, N. S.; Thompson, M.; Davis, J.; Jiang, L.; Jones, T. G. J.; Compton, R. G. *Mikrochim. Acta* **2001**, *137*, 105.
(28) Lawrence, N. S.; Wadhawan, J. D.; Compton, R. G., *Foundations of Physical Chemistry*: *Worked Examples*; Oxford University Press: Oxford, 1999; pp 140−2.
(29) Ball, J. C., *D.Phil. Thesis*, University of Oxford, 2000.
(30) See for example, Lee, H. J.; Fermin, D. J.; Corn, R. M.; Girault, H. H. *Electrochem. Commun.* **1999**, *1*, 190.
(31) Lawrence, N. S.; Thompson, M.; Davis, J.; Jiang, L.; Jones, T. G. J.; Compton, R. G. *Chem. Commun.* **2002**, 1028.
(32) Marken, F.; Compton, R. G. *Electrochim. Acta* **1997**, *43*, 2157.
(33) Scholz, F.; Kormorsky-Lovrić, Š.; Lovrić, M. *Electrochem. Commun.* **2000**, *2*, 112.
(34) Kormorsky-Lovrić, Š.; Lovrić, M.; Scholz, F. *J. Electroanal. Chem.* **2001**, *508*, 129.
(35) Gulaboski, R.; Mirčeski, V.; Scholz, F. *Electrochem. Commun.* **2002**, *4*, 277.
(36) Gergely, A.; Inzelt, G. *Electrochem. Commun.* **2001**, *3*, 753.
(37) Donten, M.; Stojek, Z.; Scholz, F. *Electrochem. Commun.* **2002**, *4*, 324.
(38) Wadhawan, J. D.; Marken, F.; Compton, R. G. *Pure Appl. Chem.* **2001**, *73*, 1947.
(39) THPD is less dense than the aqueous solution. A crude estimate of the density is ca. 0.93 g cm^{-3}
(40) This is contrary to what was reported earlier (ref 11). This is probably due to an instrument artifact—see for example ref 15; the data reported in Figure 8c were recorded using an analogue instrument.
(41) See for example Hammereich, O.; Parker, V. D. *Adv. Phys. Org. Chem.* **1984**, *20*, 55.
(42) Nickel, U.; Borchardt, M.; Bapat, M. R.; Jaenicke, W. *Ber. Bunsenges. Phys. Chem.* **1979**, *83*, 8773.
(43) Nickel, U.; Jaenicke, W. *Ber. Bunsenges. Phys. Chem.* **1982**, *86*, 695.
(44) See for example http://dcwww.epfl.ch/cgi-bin/LE/DB/InterrDB.pl This is a very good compendium of Gibbs energies for ion transfer across liquid|liquid interfaces complied from a variety of literature sources by Hubert Girault, Ecole Polytechnique Fédérale de Lausanne.
(45) See for example Greenwood, N. N.; Earnshaw, A. *Chemistry of the Elements*; Pergamon Press: Oxford, 1984.
(46) Savéant, J.-M. *J. Phys. Chem. B*, **2001**, *105*, 8995.
(47) (a) Krienke, H.; Barthel, J. *Exp. Thermodyn.* **2000**, *5*, 751. (b) Dupont, J.; Consorti, C. S.; Spencer, J. *J. Braz. Chem. Soc.* **2000**, *11*, 337.
(48) Wadhawan, J. D.; Marken, F.; Compton, R. G., unpublished results, University of Oxford, 2000.
(49) Terui, N.; Nakatani, K.; Kitamura, N. *J. Electroanal. Chem.* **2000**, *494*, 41.
(50) Marcus, Y. *Pure Appl. Chem.* **1983**, *55*, 977.
(51) Workentin, M. S.; Parker, V. D.; Morkin, T. L.; Wayner, D. D. M. *J. Phys. Chem. A* **1998**, *102*, 6503.
(52) Magnus, P.; Lacour, J.; Weber, W. *J. Am. Chem. Soc.* **1993**, *115*, 9347.